D.I.S.C:
Demonstrations of In Space Coatings

Team Members

Jason Lu, Nicholas Luis, Miguel Moya, Nicholas Sernberger, Noah Smargiassi, Kaiden Smith, Luke Verdi

Advisors

Sara Lego, Brian Holt, Dr. Douglas Wolfe

Abstract

This report presents the final project developed by Team Eta Leonis for the COSMIC Capstone Challenge, documenting the design, analysis, and verification work completed throughout the course of the year. The mission objective is to develop an autonomous system capable of applying high-quality thin-film coatings to small objects in orbit. This capability is essential for extending spacecraft lifetimes and improving performance, and currently no in-space reapplication method exists. This capability is achieved through three distinct operations: object manipulation, application of coatings, and surface characterization. The payload, housed on the 444W dual-array Venus X-Class Bus and being launched through the Falcon 9 rideshare program, consists of two robotic mechanical arms, two telescoping arms, two custom crucibles, a camera, a laser interferometer, a light emitter/receiver, heat piping, a radiator, and thermal insulation. The team conducted trade studies to refine the payload design and select properties such as coating/crucible materials, heating methods/control, as well as astrodynamic, data handling, and communication systems. The structural design of the payload was optimized to balance mass with mechanical robustness, and power and mass budget assessments ensured compliance with spacecraft and launch vehicle constraints. This technology demonstration will pave the way for future ISAM missions and innovations, allowing for the manufacturing of hardware in space while maintaining necessary protection from the space environment.

Sara Lego - Professor of Aerospace Engineering at Penn State, ses224@psu.edu
Brian Holt - CEO of Exotrail, brian.holt@exotrail-us.com
Dr. Douglas Wolfe - AVP of Research at Penn State, dew125@psu.edu

Introduction

While in orbit, spacecraft are subject to the extreme space environment, including temperature fluctuations, intense radiation, erosion from atomic oxygen, and micrometeoroid impacts. As ISAM capabilities continue to advance, the need for in-orbit surface treatment and coating processes becomes increasingly evident. Currently, spacecraft and components manufactured in orbit lack the ability to undergo protective or functional coatings that shield them from the space environment. Furthermore, our research identified that manufacturing of thin-film coatings is an underdeveloped field in space, despite significant advantages in coating qualities that are achievable in the ultra-high vacuum of 10^{-7} torr. This factor is important because the vacuum in space is orders of magnitude better than what commercially available vacuum pumps can produce on Earth. The goal of our mission is to prove the effectiveness and capability of applying thin-film coatings of Chromium and Aluminum inside our payload in low Earth orbit (LEO). In order for ISAM to be beneficial in the future, these thin-film coatings will need to be applied in space.

The core technology that our payload is based on is the thermal evaporation coating process, a subset of the physical vapor deposition (PVD) method. The evaporation process involves heating a crucible containing the target material in a vacuum environment until it turns into a gas. The gaseous atoms then condense onto a target surface, forming a thin metallic film. The understanding of this process was verified and enhanced by the Assistant Vice President of Research at Penn State, Dr. Wolfe. Evaporation was highlighted for its rapid deposition rate, technological maturity, and simplicity, making it an attractive option for space applications, and two materials were chosen based on material properties specific for in-space applications and confirmed through a trade study. Aluminum was chosen for its high reflectivity to visible and near-infrared wavelengths, and chromium was chosen for the stability of its oxide layer to act as a shield against atomic oxygen in LEO. Our comprehensive research into thermal evaporation coatings, material properties, and application techniques provided the technical foundation for our design concepts. By identifying the coating process to be used, material capabilities, and material characterization methods, our conceptual designs met the demands of our innovative mission in various ways.

Mission Overview

By assessing the required functions laid out in the functional architecture, as well as the Request for Proposal (RFP) put out by COSMIC, the team was able to form a list of top-level requirements for the payload. These requirements are expanded upon in more detail in the Eta Leonis SRR document.

1. The payload shall analyze the surface of the object prior to coating.
2. The payload shall move the target object within the payload.
3. The payload shall coat the surface of the object with a thin metal film.
4. The payload shall analyze the surface of the object after the coating is complete.

5. The payload shall be compatible with the Venus X-Class Spacecraft.
6. The payload shall abide by all relevant governmental regulations.

To ensure that the payload meets all mission requirements, each team member is tasked with overseeing the development of the various subsystems outlined in the System Decomposition, as shown below:

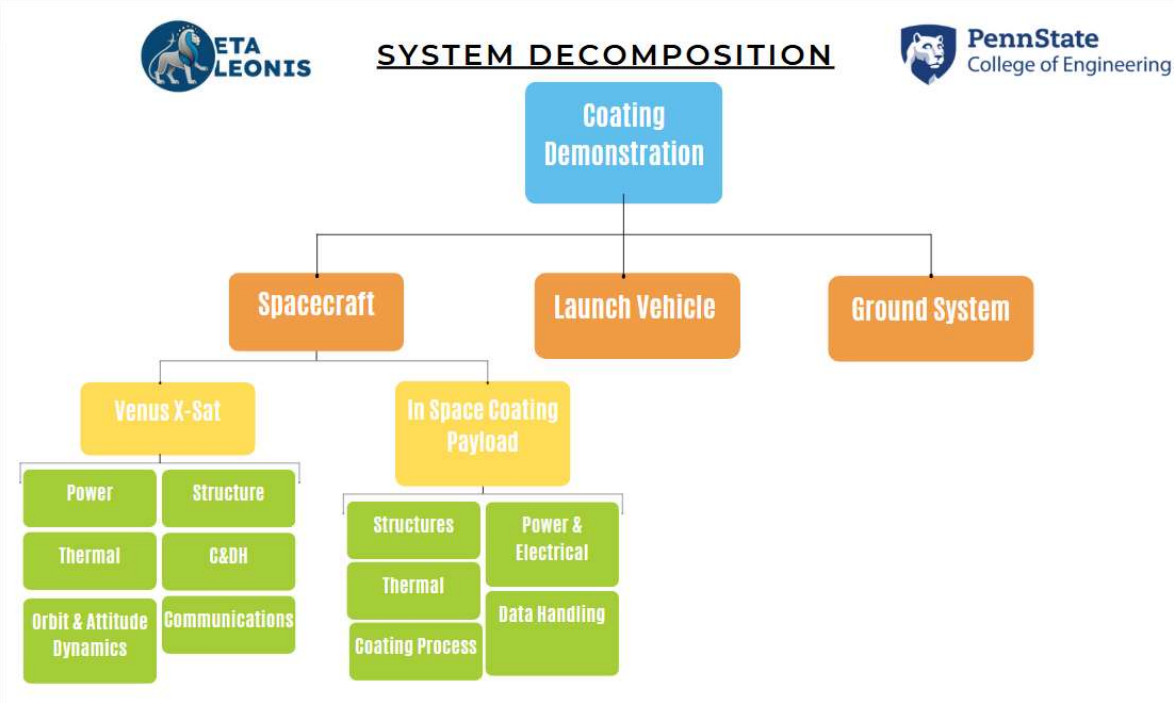

Figure 1. Systems Decomposition.

The system decomposition diagram for the Coating Demonstration project presents a hierarchical breakdown of the entire system into its constituent subsystems and clearly outlines the associated responsibilities. At the highest level, the project is segmented into three main components: the BCT Venus Class Bus, the Payload, and the Launch Vehicle. The BCT Venus Class Bus further divides into Propulsion and Attitude/GNC functions, with the latter detailing subcomponents such as Power/Electrical (led by Luke) and Communications (led by Nick Sern). The Payload component is split into the Coating Process, overseen by Nick Luis, and Thermal Management, guided by Noah. Finally, the Launch Vehicle is focused on Structures, under the leadership of Miguel and Jason. This organized decomposition not only clarifies the project's structure but also delineates clear lines of responsibility, enabling a focused approach to managing the intricate details of the mission.

Below is a diagram for the macro-level mission architecture:

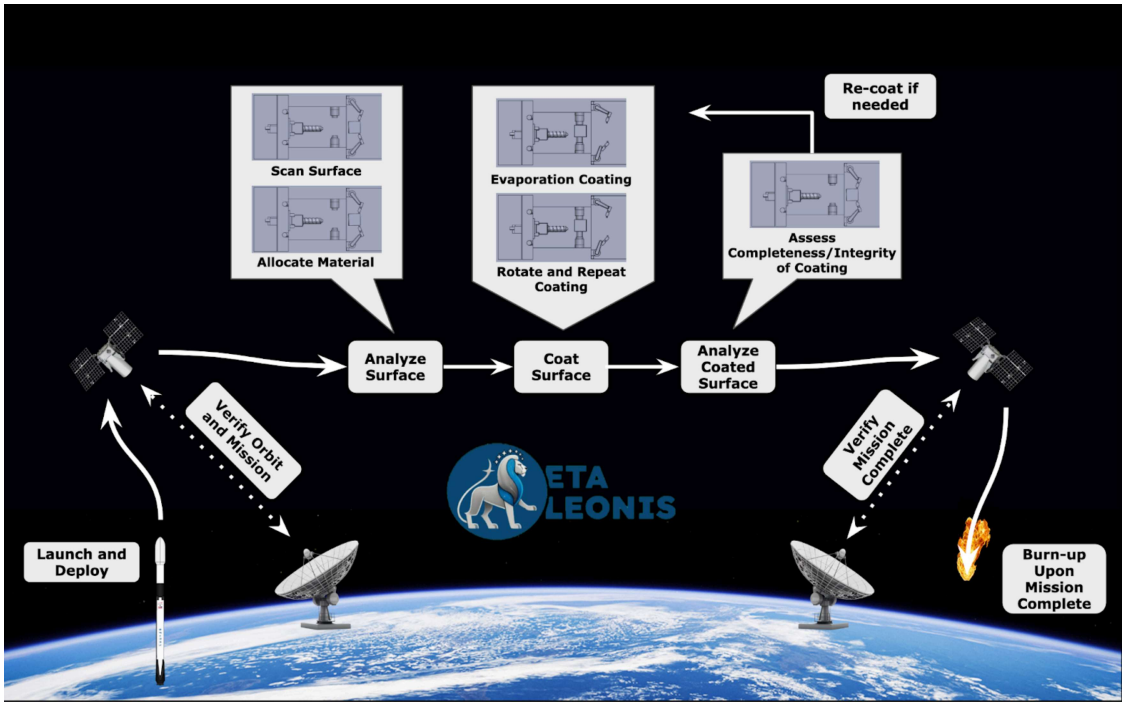

Figure 2. Macro-Level Mission Architecture.

To begin its life cycle, the payload is launched and deployed into its operating orbit. Operations begin with the twin robotic arms transferring the object to the telescoping arms. Next, the telescoping arms move the substrate into the coating position. Once maneuvered into place, the payload surface undergoes an initial scan to assess its condition before the coating application. The information obtained from this pre-coating scan is recorded and processed by the onboard computer before being transmitted to a ground station. The desired coating is then applied using an evaporation method. Once the coating process is complete, a subsequent scan verifies the quality of the coating, ensuring it meets the required material specifications. The payload will then enter a waiting period as the payload cools from its coating crucible temperature of 1650 °C. Once cooled, the telescoping arms will rotate to the opposite side of the object. The crucibles will move along the slider to coat with the second material. This follows the same steps as the first coating. This process is repeated over the life cycle of the payload. At end-of-life, the payload will shut down all primary systems and maneuver itself to a standard graveyard orbit.

Payload Design

Since the original CONOPS designs for the payload, Eta Leonis has decided to go with an internal coating design, which was chosen based on a design-analysis trade study. This method is designed to entrap an object in an interior compartment before coating it to provide a controlled environment. A three-view and isometric rendering of the payload is shown in Figure 3.

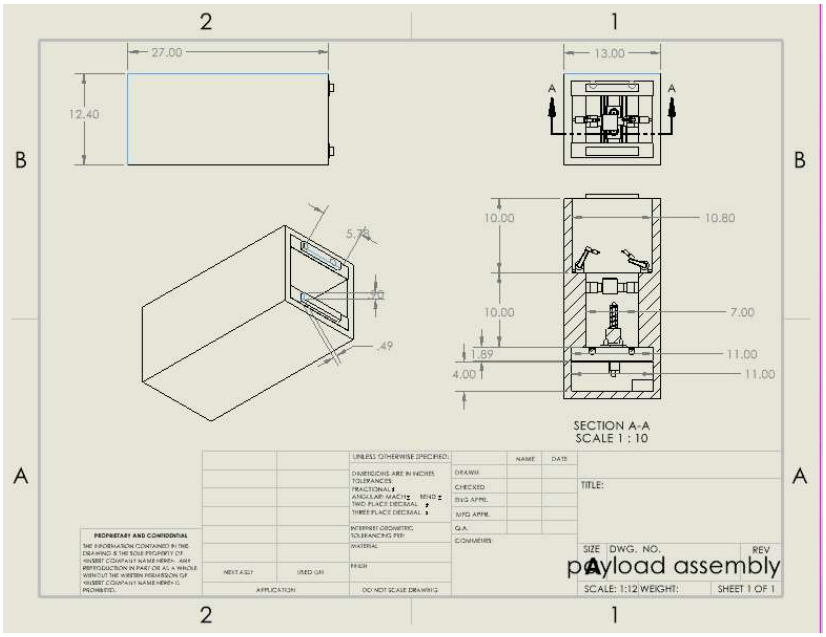

Figure 3. Payload 3-View and Isometric Rendering.

A micro-level mission architecture demonstrating the payload's operations is shown in Figure 4. The payload will be launched with one object inside of it. The object will be secured in front of a sensor and select the material that will be used for coating. The sensor will then analyze the surface for any irregularities before coating. If the object's surface has no irregularities, the crucible will be heated up by a spiral coil, evaporating the material inside, depositing it on the surface of the object. After the coating is complete, the sensor will rescan the object's surface to find any irregularities in the applied coating, and if no irregularities are found, the object will be sent out of the payload.

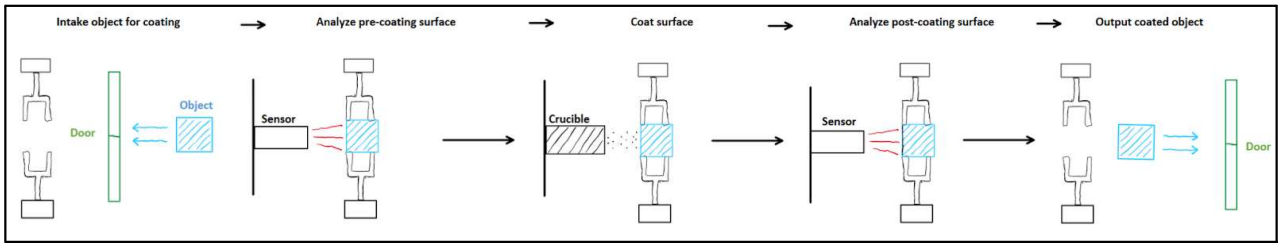

Figure 4. Micro-level Mission Architecture.

The payload for the Eta Leonis in-space coating mission has been designed as a semi-autonomous system focused on the application of thin-film coatings in orbit, addressing the ISAM capability gap. The payload is engineered for seamless integration with the Venus X-Class Bus and is optimized to meet mass, volume, and power constraints specified by the COSMIC Capstone Challenge. The design emphasizes operational efficiency in microgravity, durability in the space environment, and autonomy to reduce crew intervention during coating operations.

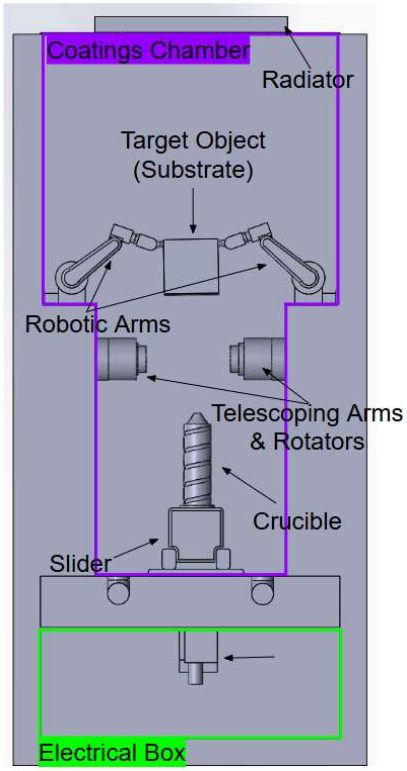

Figure 5. Payload components.

The payload is housed within a rectangular structure measuring 23” x 13” x 12.4” and is fabricated from 7075 aluminum alloy for its high strength-to-weight ratio and space-grade durability. The internal design features an electrical control box, a coating chamber, and an intake/return hallway for the transfer of objects. The payload includes a fully integrated thermal management system, heat pipes, and radiators to dissipate heat generated during the coating process. At the heart of the system is the coating chamber shown in Figure 5, where thin-film coatings are applied using the evaporation method. Prior to and following the coating process, objects are analyzed via an integrated surface characterization module featuring a laser interferometer, white light emitter/receiver, and image recognition camera to verify coating quality and material properties.

Payload Design - Structures

The Primary payload structures shall consist of a lattice of 2” X 2” Al 7075 alloy beams arranged around the payload’s interior volume. Structural supports shall be primarily designed to allow the payload to survive the high compressive load and vibrations associated with launch. Therefore, structural components are designed to withstand maximum compressive force along the payload’s primary axis only. The structural component load resistance shall be measured using a column buckling software simulation to verify the survival of the launch. A similar software analysis shall be performed for the structural components’ resistance to vibration. The payload’s structural subsystem also supports several internal and external fastener points to both

mount the payload to the BTC Venus-Class Bus and mount all other internal/external payload subsystems. Internal mounting shall use standard bolt fastenings for payload mounting. Bus mounting shall be designed to meet the design specifications provided by BTC for the Venus Class Bus.

The estimated mass of the structural subsystem is 21.0 kg. This includes approximately 12.0 kg for the main aluminum frame, 4.0 kg for internal rails and brackets supporting subsystems, 2.0 kg for bus mounting hardware, 1.0 kg for fasteners and bolts, and 2.0 kg as margin for welding materials, adhesives, and localized reinforcements. This updated structural mass accounts for roughly 36.5% of the total payload mass of 57.6 kg. While this is slightly above the original 30% guideline, the increase is justified by the need to thermally isolate the high-temperature coating chamber (up to 2500°C) and support the robotic arms that maneuver objects within the payload. The full mass budget can be found in Table 1.

Table 1. Mass Budget.

Subsystem	Component(s)	Estimated Mass (kg)
Structures	Aluminum 7075 frame and support lattice	21.0
Coating Process	Crucibles, robotic arms, telescoping arms, slider	16.5
Thermal System	Heat pipes, radiators, heat shields, insulation	5.0
Surface Characterization	Camera, laser interferometer, photodiode sensor	3.0
Command & Data Handling	KP Labs Antelope OBC, cabling, sensors interface	1.5
Power Subsystem	Li-ion batteries, harnesses	2.0
Mounting Hardware	Bolts, brackets, fasteners	1.0
Contingency Margin	(15% of subtotal above)	7.6
Total Estimated Payload Mass		**57.6**

Payload Design - Object Manipulation

The object manipulation of the payload is responsible for securely handling target objects before, during, and after the coating process. This system enables autonomous and precise positioning of substrates within the coating chamber to ensure proper alignment and uniform film deposition. The manipulation system consists of two main components: robotic arms and telescoping arms, each playing a distinct role in executing the payload's coating operations.

The robotic arms shown in Figure 6 selected for the payload are modeled after the Mitsubishi RV-2AJ industrial robot arm. These arms offer five degrees of freedom, allowing them to maneuver in complex trajectories and securely grasp the target object from the intake hallway. Their multi-jointed configuration supports flexible motion, including lifting, rotation, and angular adjustment, which are essential for precise positioning of irregularly shaped or non-cooperative payloads. These arms are mounted inside the coating chamber and can reposition objects both before and after the coating sequence.

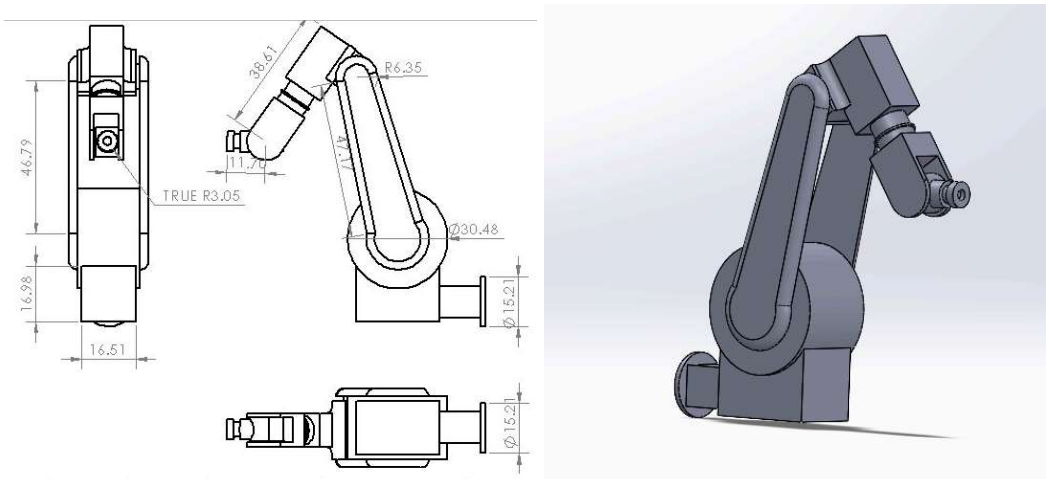

Figure 6. Mechanical Arms

Complementing the robotic arms are the telescoping arms shown in Figure 7, which provide two degrees of freedom: one translational direction and one rotational direction. These components enable fine-tuned adjustment of the object's distance relative to the crucible and help maintain consistent spacing for optimal coating thickness. The telescoping arms also feature active thermal management, utilizing embedded cooling systems to prevent overheating when operating near the high-temperature crucible that reaches temperatures in excess of 1650°C. This cooling is critical to preserving actuator function and ensuring safe, sustained operations in the chamber's thermally aggressive conditions. Together, the robotic and telescoping arms enable the payload to autonomously retrieve, position, and release target objects throughout the coating process.

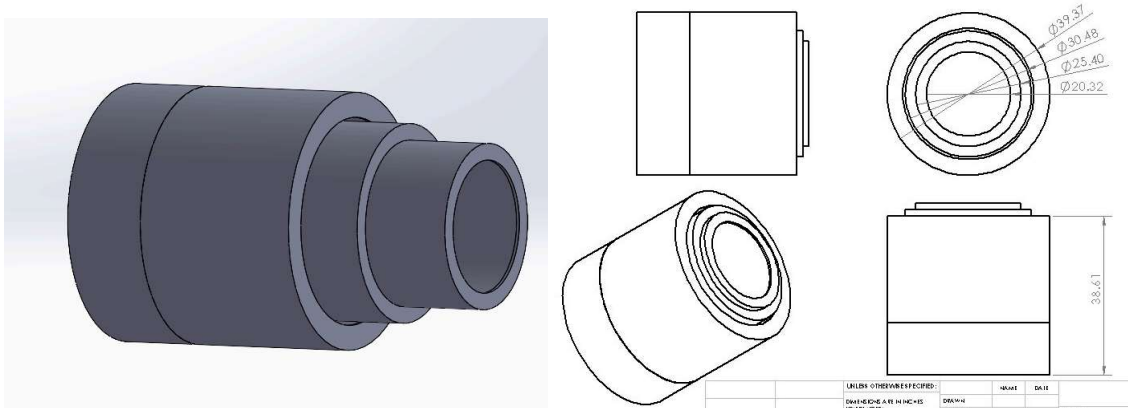

Figure 7. Telescoping Arms

Payload Design - Surface Characterization

Analyzing, or characterizing, the surface both before and after the coating process is a requirement to verify that the coating process has succeeded. Specifically, three properties needed to be measured: surface roughness, reflectivity, and visual appearance. Thus three types of sensors were needed to obtain this data: a laser interferometer to measure roughness, a white

light emitter/receiver to measure reflectivity, and an HD camera to obtain an optical image. The laser interferometer makes use of the property of waves: the magnitudes of the waves add up when they are in-phase but cancel out when they are out of phase. While the exact mechanisms of how this is achieved is beyond the scope of this report, it's worth noting that the instrument can measure surface roughness up to a resolution of half the wavelength of light being used. This payload will use a standard red laser diode, which emits a 650 nm wavelength. This means that the instrument will be able to measure surface roughness up to 325 nm, or 325×10^{-9}m. The phot-electric sensor measures the reflectivity of a surface by emitting a light and measuring the amount of light that has returned to the sensor. Finally, the camera simply functions as a normal photo camera, which needs no explanation.

These sensors are common within the materials characterization industry, so they can be obtained via commercial sources. These sources often provide a "spec sheet" that details useful information like the power and temperature requirements. Though these vendors do not design these sensors for the extreme temperatures and radiation in space, it provides an added margin of safety by designing the spacecraft around these more susceptible sensors. In the future, it is recommended that radiation-hardened electronics be custom-made specifically for this mission. Figures 8 through 10 below show CAD models of the different sensors being used, each of which are modeled after a current commercially-available sensor or technology.

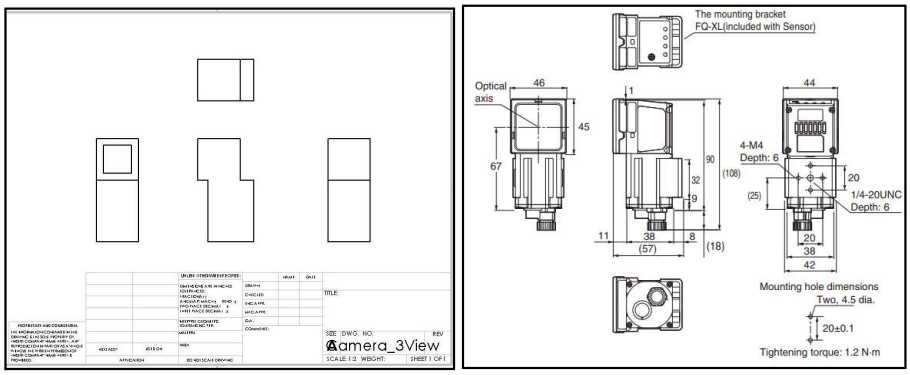

Figure 8. CAD design of the camera sensor (left), modeled after the FQ2 camera made by the OMRON Corporation (right).

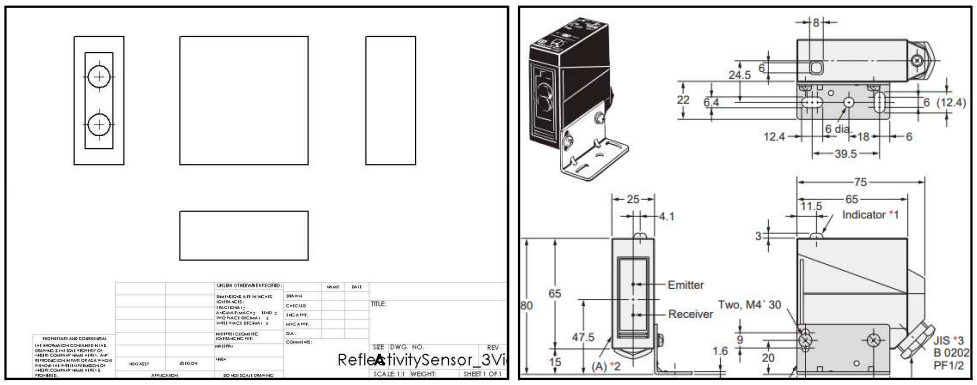

Figure 9. CAD design of the photo-electric sensor (left), modeled after the E3JK sensor made by the OMRON Corporation (right).

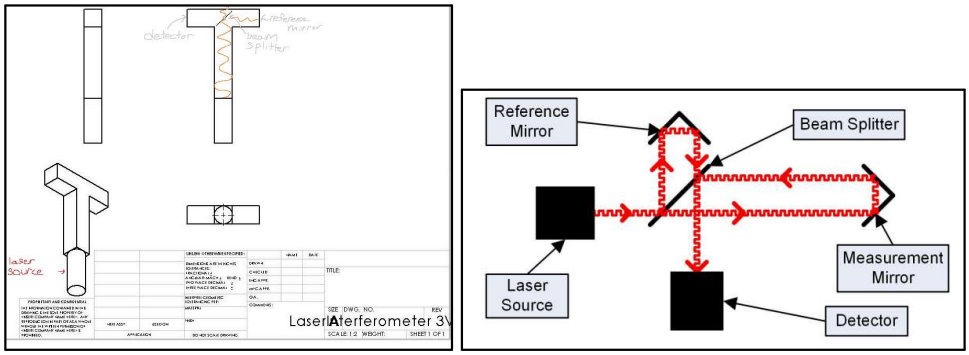

Figure 10. CAD design of the laser interferometer (left), modeled after a conceptual diagram (right) made by Dr Jody Muelaner on Engineering.com.

With these three sensors, the surface can be analyzed in a quantitative way. The data is then automatically processed on-board the spacecraft computer to determine if the coating had succeeded. For the purpose of this conceptual design, it has been assumed that sufficient data has already been collected to enable the computer to automatically determine the quality of the coating. For example, the onboard computer will automatically declare an aluminum coating a success if the reflectivity is measured to be greater than some threshold, which has been defined via on-the-ground testing.

Payload Design - The Coating Process

One of the mission requirements is to coat using the evaporation process. This was chosen because it is a simple, well-understood, and mature technology. Typically, it does not require any moving parts, but our payload will have both the coater and the target surface, or substrate, moving around to deposit an even layer. This is because the thickness of the coating is governed by the following equations compiled by Vossen and Kern [1, p.85]. Knudsen's cosine law is

$$\frac{t}{t_0} = \frac{1}{[(1+x/h)^2]^2} \tag{1}$$

where t and t_0 are the thicknesses vertically below the evaporation source at a distance h and at a radial distance x from the vertical line, respectively. Similarly, the rate of evaporation is described by the Hertz-Knudsen equation as follows:

$$\frac{dN_e}{A_e dt} = \alpha_v (2\pi mkT)^{-1/2}(p^* - p) \tag{2}$$

where α_v is the evaporation coefficient, $dN_e / A_e dt$ is the number of molecules evaporating from a surface area A_e in time dt, p^* is the equilibrium vapor pressure, p is the hydrostatic, m is the molecular weight, k is Boltzmann's constant, and T is the absolute temperature. Note that the hydrostatic pressure p is approximately zero in space. Also, the evaporation coefficient α_v is

assumed to be 1, but it can be anywhere from 0-1 depending on the “cleanliness” of the surface that is being evaporated [1]. With these equations, it was determined that the coater should move at 1 cm/s to deposit a coating that is 30µm thick in 1 second. This coating thickness and high deposition rate were identified by Sennet and Scott [2] for manufacturing a smooth and even coating. Furthermore, it was calculated that the coatings should be applied in straight lines that are spaced 1.64cm apart to generate a smooth coating.

There are many ways to evaporate a material. In fact, the materials don’t even need to reach their vaporization temperature, also known as its boiling point. Metal atoms near the surface can randomly have enough energy to escape as a gas, despite the bulk of the material being lower than the boiling point. This random evaporation increases exponentially with temperature and their “vapor pressure” is known [3]. The coating process for this mission was designed to operate at 1,650°C as a balance between thermal management and sufficient evaporation. The coating industry currently uses many different sources, such as electron beams, lasers, or resistive heating to get a material up to its vaporization temperature. From a trade study analysis, the resistive heating method was chosen, which works by simply passing a large current through a wire to generate heat through the resistivity in the wire. However, should any molten metal freely float inside the payload, it can interfere with mechanical and electrical components. Thus, a special crucible was designed. This can be seen in Figures 11 below. It was designed with a small opening at the top for the gaseous, vaporized metals to escape. As a further contingency, it was designed to be tall and skinny so as to allow the molten metals to adhere to the walls. Along the outside of the crucible is a groove that allows for a coil of wire to be wrapped around and heat the crucible via the aforementioned resistive heating method.

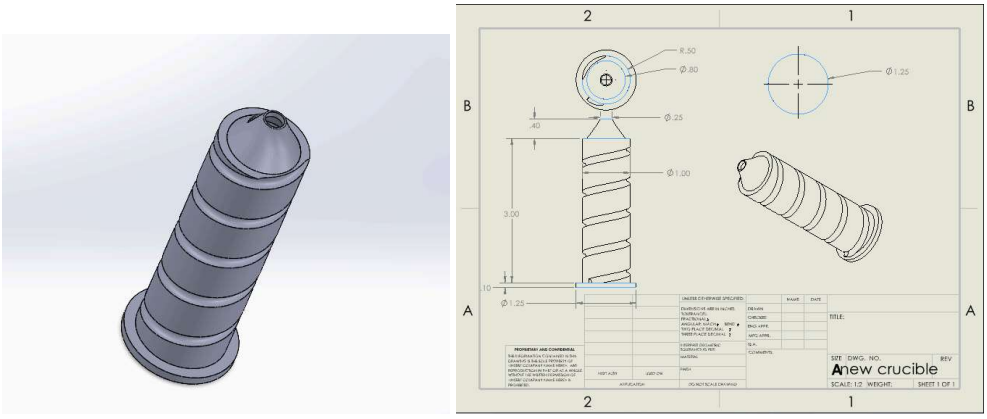

Figure 11. (left) Custom-made crucible. (right) 3-View of the custom-made crucible.

Payload Design - Thermal Subsystem

The thermal subsystem is a critical component designed to manage extreme temperature conditions of up to 1650 °C during the payload’s operation. A robust thermal control strategy to protect sensitive instruments, maintain the temperature of structures, and efficiently dissipate the excess heat is required to ensure operational stability. To satisfy the requirements for the payload, two heat shields surround the crucible, heat pipes are located in each hallway to transport heat,

radiators are used to effectively dissipate excess heat, thermostats are used to monitor temperatures, and heaters and coolers are used to maintain thermal stability in the electrical box and hallways.

The thermal subsystem is designed based on the operational limitations of the electronics. Specifically, the surface characterization sensors need to operate between -10C to +50C, according to the commercial sources of these sensors. The design also uses a worst-case scenario assumption where the crucible is heated to its maximum temperature. The total heat that the crucible emits is 9627.039 watts.

The heat shields surround the crucible, leaving a 0.05-inch vacuum gap between each structure. The vacuum gap allows for all heat transfer by radiation. The primary heat shield is made of Molybdenum, and the secondary heat shield is made of Yttria-Stabilized Zirconia. Both materials are selected due to their high melting point and low emissivity[4][5]. The heat that is not emitted through the shields is reflected back into the crucible. This allows the payload to operate using a minimal power of 400 W.

Attached to the wall separating the coating process with the hallways are space copper-water heat pipes chosen for their high heat flux capacity of 50 W/m^2. These transfer the excess 400 W emitted from the heat shields to radiators located near the payload doors. The radiators dissipate the excess heat to deep space.

Within the hallways and the electrical box are thermostats that monitor the temperature experienced within that location. When the thermostats in the hallways read a temperature outside of the -10C to 50C range, they automatically activate or deactivate until the desired temperature range is reached.

Payload Design – Command & Data Handling

For the command and data handling subsystem, we will be including an onboard computer in our payload design, in addition to defining the flow of commands to the payload and subsystems. The only requirements for the onboard computer are for it to be resistant to radiation, fit the mass/power budget, and have the necessary storage/processing power for the mission duration. The computer will be housed within the payload, a decision determined through research conducted to find high-quality computers built for small satellites. From a list, we identified KP Lab's Antelope, Spaceteq's OBC-GR712, STM Defense International's NANOSAT PRO, and AAC Clyde Space's SIRIUS OBC LEON3FT. A trade study on these four onboard computers was completed to determine which was to be included within the payload. The four primary categories in which each computer was analyzed were mass, power consumption, flight heritage, and common applications. Mass was the most important consideration to keep the mass allocated to the C&DH subsystem to a minimum. Power consumption and common computer applications were weighted above the minimum as fitting into the power budget, and a computer tested in similar mission applications were important considerations. The category with the least weight was flight heritage as this show of reliability is vital, but all four of the studied computers had excellent flight heritage. Data from the trade

study is based on each computer's data, found from [6],[7],[8],[9] respectively. The clear winner from the study was KP Lab's Antelope sat. onboard computer. Not only does this unit fit into the mass and power budgets for our payload, but it contains 12-16 GB of storage and has application history in S/X Band communication, telemetry, tracking, and commands.

The second portion of work completed for the C&DH subsystem is defining the flow of commands within the spacecraft. The only commands to be transmitted for the mission are to move the object into the coating position, begin the coating application, and transmit data to the ground station during the next available communication window. The flow chart is detailed below in Figure 12.

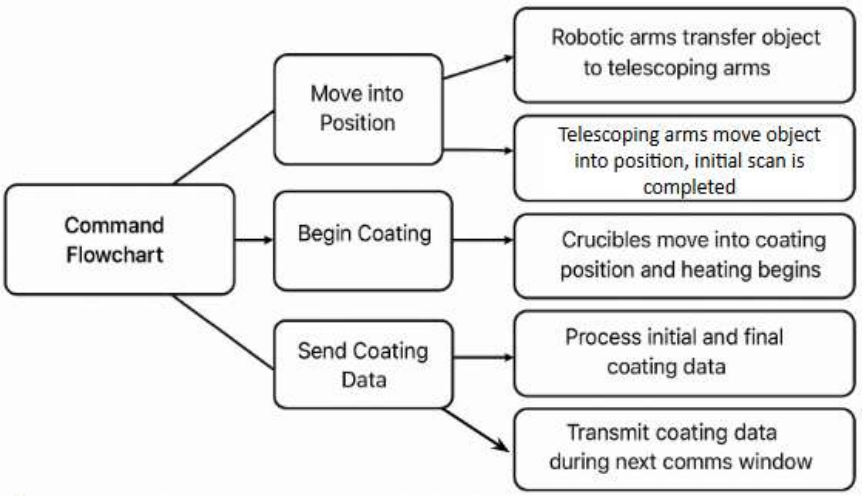

Figure 12. Command Flowchart.

Payload Design - Power

The two main concerns for the power subsystem were the secondary battery and the power budget. For the battery, a Li-ion battery was chosen because it boasts better specifications [10, Table 21-18] than other industry-standard types. For which Li-ion battery to use, a trade study was done comparing four different batteries from two different companies [11-14].

Table 2. Secondary Battery Trade Study.

Battery Name, Company	Weight	Goal	43 Ah, EaglePicher	60 Ah, EaglePicher	28-Volt Modular, Ibeos	SmallSat, Ibeos
Capacity (Ah)	**0.05**	**MAX**	**43.00**	**60.00**	**29.46**	**5.08**
Normalized value			0.69	1.00	0.44	0.00
Storage (Wh)	**0.20**	**MAX**	**154.80**	**216.00**	**825.00**	**135.00**
Normalized value			0.03	0.12	1.00	0.00
Max Discharge Rate (A)	**0.40**	**MAX**	**200.00**	**250.00**	**60.00**	**10.00**
Normalized value			0.79	1.00	0.21	0.00

Max Charge Rate (A)	**0.10**	**MAX**	**21.50**	**12.00**	**15.00**	**2.50**
Normalized value			1.00	0.50	0.66	0.00
Volume (cm^3)	**0.15**	**MIN**	**897.07**	**1,514.23**	**4630.50**	**418.40**
Normalized value			0.89	0.74	0.00	1.00
Mass (kg)	**0.05**	**MIN**	**1.27**	**1.60**	**5.90**	**0.82**
Normalized value			0.91	0.85	0.00	1.00
Temperature Range (°C)	**0.05**	**MAX**	**80.00**	**60.00**	**45.00**	**45.00**
Normalized value			1.00	0.43	0.00	0.00
Totals:	**1.00**		**0.69**	**0.70**	**0.37**	**0.20**

For the power budget, shown in Table 2, each subsystem's max power draw was found and compiled together to see if the payload would be able to sustain the maximum amount of power draw it could ever experience. A further power profile is shown in Table 3.

Table 3. Power Budget.

Subsystem	Peak Power Consumption (Coating Inactive) (W)	Peak Power Consumption (Coating Active) (W)
Evaporation Coating	0.0	415.0
Propulsion	0.0	0.0
Thermal	22.2	22.2
Structures	0.0	0.0
Power	4.9	4.9
CD&H, Uplink, & Downlink	14.0	14.0
Attitude Control	23.5	0.0
System Reserve (20%)	88.8	238.8
Battery Charging	290.6	0.0
Total Power Used	**444.0**	**694.9**
Solar Panel Power Generation	444.0	444.0
Battery Power Generation	0.0	750.0
Total Power Generation	**444.0**	**1194.0**

Spacecraft Bus Design - Guidance, Navigation, and Control (GNC)

The GNC subsystems required for the Venus Bus consist of a star tracker, reaction wheels, and an overarching attitude control system (ACS). All of this equipment will be housed

within the bus and, therefore, will not occupy any of the payload space or weight. This design assumption, as well as the specific equipment selections, came from the Venus Bus's data and components sheet in which BCT laid out the capabilities of the bus itself and the different GNC systems they provide. Using the options given by BCT, trade studies were conducted in which different properties of each system were weighted, and the values were normalized and scored to find the best possible option in each category.

For the star tracker, the biggest considerations were the Sun and Earth baffle exclusion angles. These are the angles in which incoming light from either the Sun or Earth is excluded from the star tracker's sensors. Because the payload is operating in LEO and has no need for a large field of view for stars, having a high baffle angle is beneficial for reducing light interference. With these considerations in mind, the Standard NST star tracker [15] is the best option for the payload.

The biggest considerations for the selected reaction wheels were the maximum possible torque and the power usage at maximum momentum. The goal was to have the highest possible torque while keeping the lowest power usage, which ended up being the same values for both of the options. In the end, the best selection for our mission is the RW8 reaction wheel [16].

Finally, the assessment of the overall ACS was weighted heavily for pointing accuracy and slew cross error, the latter being the deviation of a spacecraft as it is rotating. The best option for ACS is clearly the Flex Core [17], with it having nearly half the slew error and a much higher pointing accuracy. The only notable issue it has is a significantly higher supply voltage, but that is outweighed by its strength in other parameters.

Spacecraft Bus Design – Astrodynamics

The astrodynamics subsystems primarily dealt with orbit determination and creating a model that could be used to perform calculations necessary for other subsystems. The orbit was decided by taking the halfway point between the orbit properties of the ISS and Starlink in an effort to show feasibility in both government and commercial applications. Before this decision, a sun-synchronous orbit was considered for its constant sunlight, but it was rejected as it doesn't reflect a typical orbit and wouldn't show a realistic application of the technology. In the end, the selected orbit was a circular LEO at 500 kilometers with an inclination of 52 degrees. The altitude was chosen as a rough midpoint between the ISS (460km) and Starlink (550km), and the inclination was selected to almost match the ISS (51.6 degrees) and be able to easily take off from the launch site at Kennedy Space Center.

Analysis of this orbit was performed using Ansys Systems Tool Kit (STK), in which the target orbit was propagated, and the selected ground stations were mapped. The model was used to gather data for other subsystems, such as lighting and ground station access times per orbit, and determine the feasibility of the orbit in relation to launch sites and different ground stations.

Spacecraft Bus and Mission Element Design Verification

To properly select each mission element, as well as ensure the Venus Bus was the best option for our mission, design analysis and verifications were made for each. The major selected mission elements were orbital details, ground stations, launch vehicle, and Venus Bus, all of which were verified in ways unique to their role in the payload's needs.

Orbital details were verified using the aforementioned STK model created by the astrodynamics subsystem. The model was run over a seven-day period with the payload starting over Kennedy Space Center; this was used as the basis for aspects of the ground station verification work. The four ground stations, Ohio, Ireland, Australia, and Bahrain, were selected both for their global position and their mean access time over the 7-day simulation window. The 10 MHz bandwidth was verified by BCT's information on antenna options for the Venus Bus [18]. Using the orbital model created, each ground station's average access times per orbit were calculated, and the final selections were made based on those values. The main station, Ohio, had the highest mean access time at 688.03 seconds. By ensuring that each one had sufficient access to the payload, it verified that both the ground stations themselves and the selected orbit were compatible with the mission.

The ground station locations were selected from the Amazon Web Services (AWS) ground station list, which can be found in Ref. [19]. Since our planned launch is from KSC in Florida, we needed the simulated orbit to start over this area, as seen above in Figure x. From the information provided on AWS ground system operations, we determined 5 categories to grade the BCT Venus Bus antenna options on. These five categories were frequency, gain, bandwidth, operating temp., and power usage. Based on specifications from BCT, a trade study was conducted to determine which antenna to choose for our mission. The antenna operating frequency matching the AWS ground stations had the highest weight as our mission needs to be able to transmit telemetry (commonly in S band) and payload data (X band). Based on the selected antenna, the following link budget for downlink was generated for the mission, as seen in Tables 4 and 5.

Table 4. Downlink Link Budget.

Item	Symbol	Units	Source	Cmd to orbiter
Freq.	f	Ghz	input	**8.00**
Xmtr Pwr	P	W.	input	**4.0000**
Xmtr Pwr	P	dbW	10 log(P)	6.02
Xmtr line loss	L_l	dB	input	**-1.00**
Xmtr Ant. Beamwidth	θ_t	deg	Eq. (13-19)	62.950
Peak Xmt. Ant. Gain	G_{pt}	dB	Eq. (13-20)	8.32
Xmt. Ant. Diam.	D_t	m	input	**0.04**
Xmt. Ant. Pointing Error	e_t	deg	input	**0.00**
Xmt. Ant. Pointing Loss	L_{pt}	dB	Eq. (13-21)	0.00
Xmt Ant. Gain	G_t	dB	$G_{pt}+L_{pt}$	8.32
EIRP	EIRP	dB	$P+L_l+G_t$	13.34
Prop. Path Length	S	km	input	**1.878E+03**
Space Loss	L_s	dB	Eq. (13-23a)	-175.98
Prop. & Polariz. Loss	L_a	dB	Fig. 13-10	**-0.05**
Rcv. Ant. Diam.	D_r	m	input	**5.40**
Peak Rcv. Ant. Gain	G_{rp}	dB	Eq. (13-18a)	50.52
Rcv. Ant. Beamwidth	θ_r	deg	Eq. (13-19)	0.49
Rcv. Ant. Pointing Error	e_r	deg	input	**0.05**
Rcv. Ant. Pointing Loss	L_{pr}	dB	Eq. (13-21)	-0.13
Rcv. Ant. Gain	G_r	dB	$G_{rp}+L_{pr}$	50.40
System Noise Temp.	T_s	K	input (using Tab	**135.00**
Data Rate	R	bps	input	**3500000.00**
Est. E_b/N_o (1)	E_b/N_o	dB	Eq. (13-13)	29.57
Bit Error Rate	BER	--	input	**1.0E-05**
Rqd. E_b/N_o (2)		dB	Fig. 13-9 (BPSK,	**4.50**
Implementation Loss (3)		dB	input (standard	**0.00**
Margin		***dB***	***(1)-(2)+(3)***	***25.07***

Table 5. Uplink Link Budget.

Item	Symbol	Units	Source	Cmd to orbiter
Freq.	f	Ghz	input	**4.00**
Xmtr Pwr	P	W.	input	**4.0000**
Xmtr Pwr	P	dbW	10 log(P)	6.02
Xmtr line loss	L_l	dB	input	**-1.00**
Xmtr Ant. Beamwidth	θ_t	deg	Eq. (13-19)	0.972
Peak Xmt. Ant. Gain	G_{pt}	dB	Eq. (13-20)	44.54
Xmt. Ant. Diam.	D_t	m	input	**5.40**
Xmt. Ant. Pointing Error	e_t	deg	input	**0.05**
Xmt. Ant. Pointing Loss	L_{pt}	dB	Eq. (13-21)	-0.03
Xmt Ant. Gain	G_t	dB	$G_{pt}+L_{pt}$	44.51
EIRP	EIRP	dB	$P+L_l+G_t$	49.53
Prop. Path Length	S	km	input	**1.878E+03**
Space Loss	L_s	dB	Eq. (13-23a)	-169.96
Prop. & Polariz. Loss	L_a	dB	Fig. 13-10	**-0.05**
Rcv. Ant. Diam.	D_r	m	input	**0.04**
Peak Rcv. Ant. Gain	G_{rp}	dB	Eq. (13-18a)	1.90
Rcv. Ant. Beamwidth	θ_r	deg	Eq. (13-19)	131.25
Rcv. Ant. Pointing Error	e_r	deg	input	**0.05**
Rcv. Ant. Pointing Loss	L_{pr}	dB	Eq. (13-21)	0.00
Rcv. Ant. Gain	G_r	dB	$G_{rp}+L_{pr}$	1.90
System Noise Temp.	T_s	K	input (using Table 13-10)	**135.00**
Data Rate	R	bps	input	**1500000.00**
Est. E_b/N_o (1)	E_b/N_o	dB	Eq. (13-13)	26.96
Bit Error Rate	BER	--	input	**1.0E-05**
Rqd. E_b/N_o (2)		dB	Fig. 13-9 (BPSK, R-1/2 Viterbi)	**4.50**
Implementation Loss (3)		dB	input (standard estimate)	**0.00**
Margin		***dB***	***(1)-(2)+(3)***	***22.46***

The frequency was determined from transmitting at the highest frequency necessary for this mission or sending payload data in X band or 8 GHz. To determine the power input needed to transmit a signal at this frequency, we examined the power requirements for a high gain X band amplifier, which came out to 4 watts [20]. The antenna diameter and pointing error were provided directly by BCT in their components catalog [18]. The propagation path length was calculated from the mean range of the four primary ground stations when simulating a week-long mission with the initial orbit in line with our launch location. The propagation and polarization loss comes from SMAD Fig. 13-10[10], coming out to -0.05 dB at a frequency of 8 GHz. For the ground station antennas, specifications on AWS's full system were referenced [21]. For this mission, we increased the required data rate to 3.5 MBps to allow for the transmission of photos and data generated by the payload's operations. This data rate was based on transmission of 2-5 MB photos, or larger with longer upload/download times. Based on the above specifications, the team calculated a link margin of 25.07 dB (downlink) and 22.46 dB (uplink), which is significantly higher than necessary.

The chosen launch vehicle, the SpaceX Falcon-9, was verified using the provided Rideshare user guide [22]. This comprehensive guide covers minimum compatibility for the rideshare program and the conditions the payload will experience under launch. A base

verification of the launch vehicle was determined by ensuring the fasteners of the Venus Bus were compatible with those used by the Falcon-9.

Future Work

There is still much more work that could be done with D.I.S.C. The basis of the COSMIC challenge focused on integration with the Venus X Class bus, so from the beginning, no other bus was considered. If given a less focused premise, other buses could be researched for the project, ideally larger ones to reduce the risks associated with extreme operating heats. With more time and support, full testing of the Antelope computer could be done, focused on coating applications with sensors, cameras, etc. Extensive vibrational launch testing with the Falcon 9 could also be completed to ensure the payload is sufficiently stable. If given the opportunity, all of this testing would be done in close association with BCT, or another satellite bus provider, to ensure extensive integration with their bus. Finally, it will be necessary to work closely with commercial suppliers to source or create more mission-specific components, especially because many of the components on our payload are modeled after commercially-available parts. For example, the mechanical arms would need to be improved to allow for the coating of more complex shapes, specifically it needs another rotational degree of freedom.

References

[1] Vossen, J., Kern, W., (1991) Thin Film Processes II. https://doi.org/10.1016/B978-0-08-052421-4.50007-1

[2] Sennett, R. S., Scott, G. D. (1950) "The Structure of Evaporated Metal Films and Their Optical Properties," Journal of the Optical Society of America. doi-org.ezaccess.libraries.psu.edu/10.1364/JOSA.40.000203

[3] “Vapor Pressure Data for the More Common Elements” (1957), *Radio Corporation of America Laboratories*, https://www.one-electron.com/Archives/RCA/RCA-RB/RB-104%20RCA%20Labs%201957%20Vapor%20Pressure%20Data%20for%20the%20More%20Common%20Elements.pdf

[4] Frederick, H. M., “Experimental determination of emissivity and resistivity of yttria stabilized zirconia at high temperatures,” thesis, 2008.

[5] “High-temperature heat pipe designs & manufacturing,” *Advanced Cooling Technologies* Available: https://www.1-act.com/thermal-solutions/passive/heat-pipes/high-temp/.

[6] “50 MHz SmallSat On-Board Computer,” *SIRIUS OBC LEON3FT - AAC Clyde Space | Satellite On-Board Computer (OBC)* Available: https://www.satnow.com/products/on-board-computers/aac-clyde-space/116-1154-sirius-obc-leon3ft.

[7] “On-Board Computer for Nano-Satellite Platforms,” *NANOSATPRO - STM Defense International | Satellite On-Board Computer (OBC)* Available: https://www.satnow.com/products/on-board-computers/stm-defense-international/116-1304-nanosatpro.

[8] “On-Board Computer for Microsatellites & LEO Spacecraft,” *OBC-GR712 - Spaceteq | Satellite On-Board Computer (OBC)* Available: https://www.satnow.com/products/on-board-computers/spaceteq/116-1205-obc-gr712.

[9] “Onboard Computer for Satellites,” *ANTELOPE - KP Labs | Satellite On-Board Computer (OBC)* Available: https://www.satnow.com/products/on-board-computers/kp-labs/116-1303-antelope.

[10] Wertz, J. R., Everett, D. F., and Puschell, J. J., *Space Mission Engineering: The New SMAD*, Hawthorne, California: Microcosm Press, 2015.

[11] “SmallSat Battery Datasheet,” *Ibeos* Available: https://www.ibeos.com/28v-135whr-battery.

[12] “Modular 28V Battery Datasheet,” *Ibeos* Available: https://www.ibeos.com/modular-battery-datasheet.

[13] “60 Ah Space Cell,” *EaglePicher Technologies* Available: https://www.eaglepicher.com/sites/default/files/LP33037 60Ah Space Cell 1222.pdf.

[14] “43 Ah Space Cell,” *EaglePicher Technologies* Available: https://www.eaglepicher.com/sites/default/files/LP33450%2043%20Ah%20Space%20Cell%20%200223.pdf.

[15] “Nano Star Trackers,” *Bluecanyontech.com* Available: https://storage.googleapis.com/blue-canyon-tech-news/1/2024/03/NST-2024.pdf.

[16] “Reaction Wheels,” bluecanyontech.com Available: https://storage.googleapis.com/blue-canyon-tech-news/1/2024/03/NST-2024.pdf.

[17] “Attitude Control Systems,” *bluecanyontech.com* Available: https://storage.googleapis.com/blue-canyon-tech-news/1/2024/03/ACS-1_2024.pdf.

[18] *Blue Canyon Technologies* Available: https://www.bluecanyontech.com/components.

[19] “AWS Ground Station locations,” *Amazon Web Services* Available: https://aws.amazon.com/ground-station/locations/.

[20] “X band high gain power amplifiers,” *Pasternack* Available: https://www.pasternack.com/pages/Featured_Products/x-band-high-gain-power-amplifiers.html?srsltid=AfmBOooqSRuM9lC1v95rhVApiT3xauh5WYr5eGgyFoOTL1p-Fq_g-jY3.

[21] “AWS Ground Station”, *Amazon Web Services*, Feb. 2020, https://esto.nasa.gov/wp-content/uploads/2020/03/AWS-FCD_GroundStation_Feb2020-NOS.pdf

[22] “Rideshare payload user’s guide,” *Spacex.com* Available: https://storage.googleapis.com/rideshare-static/Rideshare_Payload_Users_Guide.pdf.